Core-Level Shift of Si Nanocrystals Embedded in a SiO$_2$ Matrix

T. P. Chen,*,† Y. Liu,† C. Q. Sun,† M. S. Tse,† J. H. Hsieh,‡ Y. Q. Fu,‡ Y. C. Liu,§ and S. Fung$^{||}$

School of Electrical and Electronic Engineering and School of Mechanical and Production Engineering, Nanyang Technological University, Singapore 639798, Singapore, Singapore Institute of Manufacturing Technology, Singapore 638075, Singapore, and Department of Physics, The University of Hong Kong, Hong Kong

It is expected from existing theories that the core level of Si nanocrystals (nc-Si) embedded in a SiO$_2$ matrix should shift toward a higher binding energy as compared to that of bulk crystalline Si due to quantum size effect. Indeed, it is observed in X-ray photoemission experiments that the Si 2p core level shifts to a higher apparent binding energy by 1–2 eV for all five oxidation states of Si^{n+} (n = 0, 1, 2, 3, and 4) in the material system of SiO$_2$ containing nc-Si. However, it is found that the core-level shift is due to a charging effect in the material system. After correction for the charging effect by using C 1s binding energy due to contamination on the SiO2 surface, the core level of the oxidation state Si^{4+} is the same as that of pure SiO$_2$, whereas the core level of the isolated nc-Si with an average size of about 3 nm shifts by $\sim$ 0.6 eV to a lower binding energy as compared to that of bulk crystalline Si. It is suspected that the core-level shift of the nc-Si toward a lower binding energy is due to the influence of the differential charging between the SiO$_2$ surface layer and the nc-Si underneath.

Recently, Si nanocrystals (nc-Si) embedded in SiO$_2$ films have attracted much attention because they exhibit new quantum phenomena and have potential applications in optoelectronic and electronic devices.[1–5] One of the promising techniques for the incorporation of Si in SiO$_2$ films is Si ion implantation into SiO$_2$ films grown by thermal oxidation of Si substrate. With this technique, nc-Si is formed and isolated inside the robust SiO$_2$ matrix that provides good chemical and electrical passivation of the nanocrystals. Optical and electrical properties of the nc-Si embedded in SiO2 matrix should be different from those of bulk crystalline Si and nc-Si thin films. Photoelectron spectroscopy can be used to probe electronic and chemical structures of the nc-Si embedded in the SiO$_2$ matrix. For nanoscale particles such as nanocrystals and metal clusters, it has been frequently reported that the core levels measured with X-ray photoelectron spectroscopy (XPS) shift with the reduction of particle sizes.[6–13] Various mechanisms have been proposed to explain the size-induced core-level shift. For example, the cluster size-dependence of the Cu 2p core-level shift is explained in terms of the influence of initial- and final-state effects,[9] the Au 4f core-level shift of the supported gold clusters is experimentally found to be consistent with the size dependence of the charging energy of the clusters,[10] and the size dependence of the Si 2p core-level shift of porous silicon is explained by the bond order–length–strength (BOLS) correlation mechanism.[6] For nc-Si embedded in the SiO$_2$ matrix, the core levels of the nc-Si could be affected by not only the nanocrystal size but also the environment of the nanocrystals. In addition, photoemission-induced charging in both the SiO$_2$ and the

isolated nc-Si as well as at the SiO$_2$/nc-Si interfaces could also affect the core levels. In this work, XPS is used to study the charging effect and Si 2p core-level shifts of nc-Si embedded in the SiO$_2$ matrix.

30 nm SiO$_2$ thin films were grown on p-type Si wafers with (100) orientation by thermal oxidation in dry oxygen at 950 °C. Then Si ions were implanted into the SiO$_2$ films at the energy of 1 keV with a dose of 8 × 10^{16} cm^{-2}. The profile of excess Si in the SiO$_2$ thin film was measured with secondary ion mass spectroscopy. The implanted Si distributes from the surface to the depth of $\sim$10 nm with the maximum concentration at the depth of $\sim$5 nm, and the subsequent annealing does not change the profile significantly because the diffusion coefficient of Si in SiO$_2$ is very low. Thermal annealing was carried out in N$_2$ ambient at various annealing temperatures for different annealing times. For simplicity, here only the results of the annealing at 1000 °C for various annealing durations ranging from 0 to 100 min are presented. The mean size of the nc-Si is determined from full width at half-maximum (fwhm) of the Bragg peak after correction for instrumental broadening in the X-ray diffraction (XRD) measurement.[14] The nc-Si size obtained is from $\sim$2.5 nm for the as-implanted sample to $\sim$3 nm for the samples annealed at various temperatures for various durations. This result is similar to that of ref 15 in which it is reported that the nc-Si size slightly increases from 2.5 nm after 1 min annealing to 3 nm after 16 h annealing at the annealing temperature of 1100 °C. This very slow evolution is due to the very low diffusion coefficient of Si in SiO$_2$. XPS experiment was performed by using a Kratos AXIS spectrometer with monochromatic Al Kα (1486.71 eV) X-ray radiation. Si 2p core-level spectra were recorded at a normal emission angle. As the spectra were taken at the depth of $\sim$5 nm which is smaller than the SiO2 film thickness (30 nm), the Si substrate did not contribute to the spectra. For the study of the charging effect, C 1s spectra from the sample surface were also recorded.

---

* To whom correspondence should be addressed. E-mail: echentp@ntu.edu.sg.

† School of Electrical and Electronic Engineering, Nanyang Technological University.

‡ School of Mechanical and Production Engineering, Nanyang Technological University.

§ Singapore Institute of Manufacturing Technology.
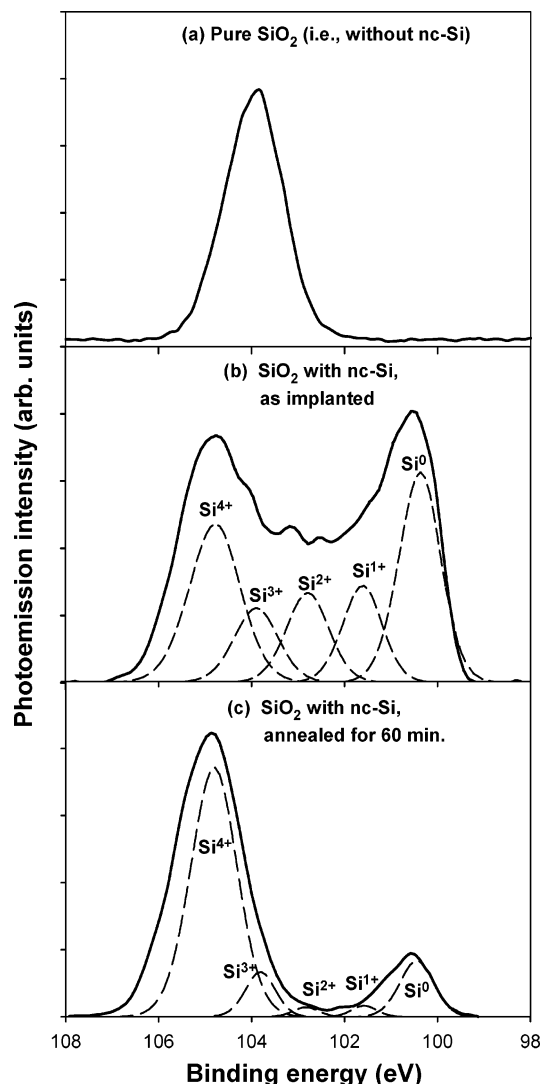
$^{||}$ The University of Hong Kong.

Figure 1. Si 2p spectra for (a) the sample without Si ion implantation (i.e., a pure SiO_2 thin film thermally grown on the Si substrate); (b) the as-implanted sample; and (c) the sample annealed at 1000 °C for 60 min. The spectra are decomposed into Si $2p_{1/2}$ and $2p_{3/2}$ partner lines for the five oxidization states without any pre-adjudication. In this figure, only the $2p_{3/2}$ components (the dashed lines) are shown.

Figure 2. Si^0 shifts relative to the Si $2p_{3/2}$ core level in bulk Si for the as-implanted sample (i.e., the annealing time is 0 min) and the samples annealed at 1000 °C for various annealing times. The binding energy of Si $2p_{3/2}$ in bulk Si is 90.0 eV (the charging effect in the bulk Si has been corrected). The solid circles represent the uncorrected shifts, and the open circles show the values after the correction for the charging effect.

Figure 1, parts a−c, shows the XPS Si 2p core level peaks for the sample without Si ion implantation (i.e., a pure SiO_2 thin film grown on the Si substrate), the as-implanted sample, and the sample annealed at 1000 °C for 60 min, respectively. It has been reported that five oxidation states of Si^{n+} ($n = 0, 1, 2, 3,$ and 4) corresponding to the five chemical structures of Si, Si_2O, SiO, Si_2O_3, and SiO_2, respectively, exist in nonstoichiometric SiO_x ($0 < x < 2$) films,[16] and they are also commonly observed at the SiO_2/Si interface.[17−19] For the Si-rich SiO_x films formed by Si ion implantation into SiO_2 films in this study, it is also reasonable to assume the possible existence of the five silicon oxidation states. With the possible existence of the five oxidation states in mind, we have carried out the curve fitting by decomposing the spectrum into the Si $2p_{1/2}$ and $2p_{3/2}$ partner lines for the 5 oxidization states without any pre-adjudication. Although the spin−orbit splitting and the Si $2p_{1/2}$ to Si $2p_{3/2}$ intensity ratio are not fixed in the fitting, the fitting yielded reasonable results. For example, for the spectrum shown in Figure 1b, the fitting yielded that the spin−orbit splitting is 0.60 ± 0.05 eV and the intensity ratio is equal to the statistical value of 1:2 within 10% for all of the five oxidation states. This is
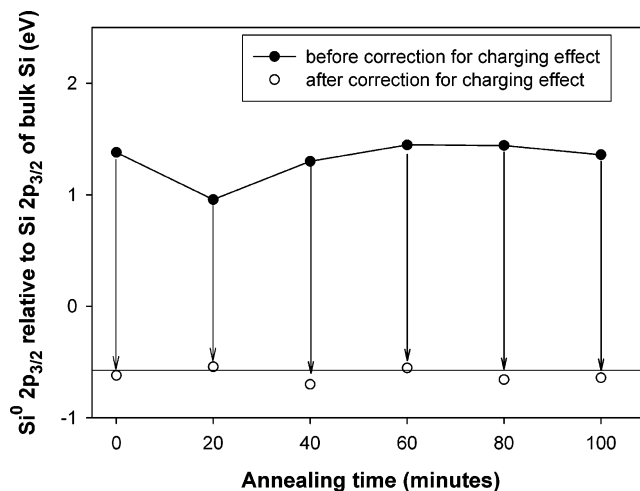
consistent with the result for SiO_2/Si system reported in the literature.[18] Such an approach has been proved to be able to provide us a reasonable picture of the changes of the chemical structures in the SiO_x film as a result of thermal annealing.

The Si 2p peak deconvolution of the above approach for the as-implanted and annealed samples is also shown in Figure 1 (for clear presentation, only the Si $2p_{3/2}$ lines are shown). The annealing-induced changes in the peak areas of the five oxidation states are due to the changes of the concentrations of the five chemical structures as a result of thermal decomposition of the suboxides (Si_2O, SiO, and Si_2O_3 corresponding to oxidation states Si^{1+}, Si^{2+}, and Si^{3+}, respectively) and oxidation of the implanted Si during the annealing. It is evident from the comparison between parts b and c of Figure 1 that the annealing causes a reduction in the Si^{3+}, Si^{2+}, Si^{1+}, and Si^0 concentrations but an increases in the Si^{4+} concentration. The reduction of the suboxides is due to the thermal decomposition of the suboxides SiO_x ($x = 1/2, 1,$ and 3/2 for Si_2O, SiO, and Si_2O_3, respectively).[20] At the same time, the oxidation of the implanted Si due to the presence of residual oxygen in the nitrogen atmosphere during the annealing leads to a decrease in the Si^0 concentration. Both the thermal decomposition and the oxidation lead to the growth of SiO_2, which explains the large increase in the Si^{4+} concentration after the annealing.

The Si 2p binding energy of the nc-Si (or Si^0) can be determined from the above peak deconvolution. The solid circles in Figure 2 represent the shifts of the Si^0 $2p_{3/2}$ apparent binding energy relative to the bulk Si $2p_{3/2}$ for the as-implanted sample (i.e., the annealing time is 0 min) and the samples annealed at 1000 °C for durations ranging from 20 to 100 min. A shift ranging from ~1 to ~1.5 eV to a higher binding energy is always observed. The situation of other oxidation states Si^{n+} ($n = 1, 2, 3,$ and 4) is also similar to that of Si^0. The solid circles in Figure 3 show the Si^{4+} shift relative to the Si 2p in pure SiO_2. As the Si nanocrystals with a size of less than 4 nm are involved, one could think that the Si^0 core-level shift is determined by quantum size effect that may originate from quantum confinement, initial- and final-state effects,[9] Coulomb charging energy,[10] surface bond contraction,[6] etc. However, as discussed below, the Si^0 shift is largely affected by the charging in the material system caused by the photoemission itself.
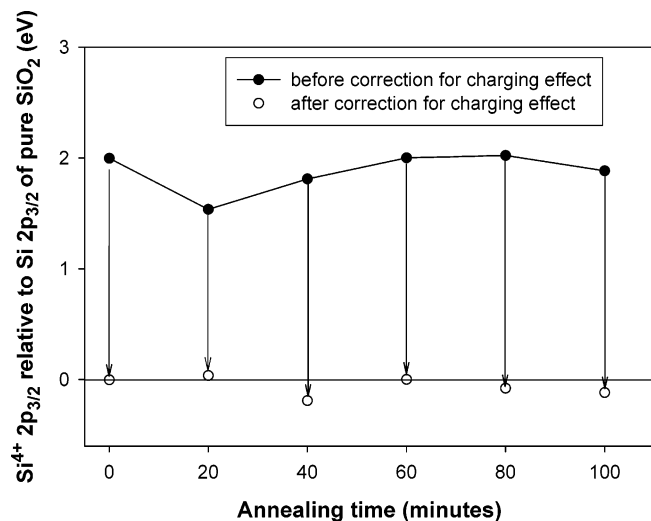
Letters

J. Phys. Chem. B, Vol. 108, No. 43, 2004 **16611**

Figure 3. Si^{4+} shifts relative to the Si $2p_{3/2}$ core level in the pure SiO_2 thin film. The binding energy of Si $2p_{3/2}$ in pure SiO_2 is 102.8 eV (the charging effect in the pure SiO_2 has been corrected). The solid circles represent the uncorrected shifts, and the open circles show the values after the correction for the charging effect.
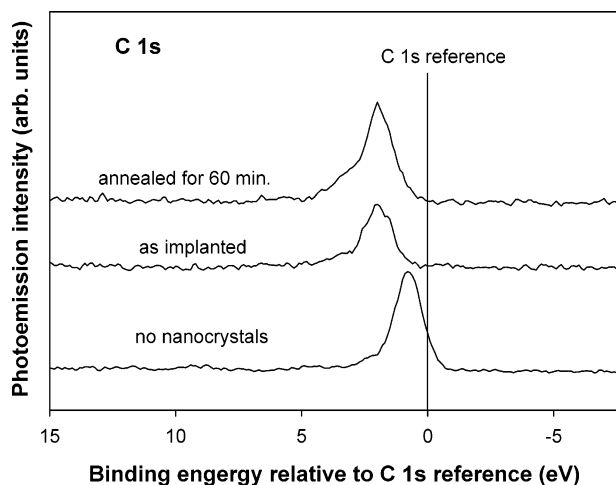

Figure 4. C 1s spectra recorded from the surfaces of the sample without nanocrystals (i.e., a pure SiO_2 thin film on the Si substrate), the as-implanted sample, and the sample annealed at 1000 °C for 60 min after the Si^+ implantation.

It has been known for a long time that under X-ray irradiation, charges can be accumulated at the SiO_2/Si interface.[17] With a large number of nc-Si embedded in the SiO_2 matrix, there should be a very large area of SiO_2/nc-Si interfaces. Therefore, in addition to the charging in the SiO_2 thin film, there is also very significant charging at the SiO_2/nc-Si interfaces. The charging will cause a core-level shift to a higher binding energy. At the same time, photoemission will also leave a charge in the nanocrystals, leading to a core-level shift to a higher binding energy also. Note that the charging in the nc-Si should be dependent on the nc-Si size. The core-level shift in the pure SiO_2 thin film due to photoemission is found to be much smaller than that in the nc-Si/SiO_2 system, indicating that the charging effect from the SiO_2 thin film is much less significant than that from the SiO_2/nc-Si interfaces and the nanocrystals.

To show the charging effect on the core-level shifts, C 1s spectra from the sample surface due to contamination were also recorded. Figure 4 shows the shifts of the C 1s core level relative to C 1s reference for the sample without nc-Si (i.e., the pure SiO_2 thin film on the Si substrate), the as-implanted sample, and the sample annealed at 1000 °C for 60 min after Si^+

implantation. The shift of the sample without nc-Si is 0.8 eV, which is due to the charging in the 30 nm SiO_2 thin film on Si substrate,[17] being much smaller than the shifts of the as-implanted and annealed samples. The shifts are in the range of ~1.5−2 eV for the as-implanted and annealed samples, showing that the charging effect is greatly enhanced by the introduction of Si into the SiO_2 matrix. The enhancement of charging effect could be due to the fact that the nc-Si and the defects at the SiO_2/nc-Si interfaces play a dominant role in the charge trapping. Actually, the application of nc-Si in memory devices relies on the excellent charge−storage capability of nc-Si embedded in the SiO_2 matrix. Note that for the samples used in this study the embedded nc-Si is confined in the region from the SiO_2 surface to a depth of ~10 nm. There is still a pure SiO_2 layer with a thickness of ~20 nm underneath this region; that is, there is a ~20 nm pure SiO_2 layer between the nc-Si region and the Si substrate. This means that it is very difficult to release the charges trapped in the nc-Si through the Si substrate.

The charging effect has an important consequence on the evaluation of the core-level shifts of nc-Si, and the correction for the charging effect must be made. As Si 2p and C 1s spectra were recorded in the same XPS experiment on the same sample, the charging effect on the Si 2p core-level shift could be corrected by subtracting the C 1s core-level shift from the raw data of the binding energy of the Si^0 2p core level. The corrections for the charging effect for Si^0 are shown in Figure 2 where the solid circles are for the raw data (i.e., before correction) while the open circles give the corrected values. A quite different picture is observed after the corrections. As shown in Figure 2, after the correction, the core level of the isolated nc-Si shifts by ~ 0.6 eV to a lower binding energy as compared to that of bulk crystalline Si, and it has no significant dependence on the annealing time. Similar corrections have been made for Si^{4+} also, as shown in Figure 3. After the correction for the charging effect, the core level of the oxidation state of Si^{4+} is the same as that of pure SiO_2 and has no significant dependence on the annealing as well.

For the nc-Si with a mean size of less than 4 nm in this study, it is expected that the nc-Si core-level would shift to a higher binding energy as compared to that of bulk crystalline Si if the quantum size effect plays a major role. The quantum size effect on the shift of the binding energy could be due to the charging energy of a single core hole in the nanocrystal,[10,11] quantum confinement, the bond order−length−strength (BOLS) correlation mechanism,[6,21] etc. When an X-ray ejects an electron out of a nanocrystal, the Coulomb interaction between the photoelectron and the hole left behind in the nanocrystal increases the binding energy by $e^2/2C$, where the self-capacitance $C = 4\pi\epsilon_r\epsilon_0 r$ when the nanocrystal is spherical with a radius of r and the surrounding dielectric has a dielectric constant ϵ_r.[10,11] For Si nanocrystals with a size of 3 nm as in the present study, the charging energy is estimated to be ~0.12 eV. On the other hand, a larger shift to a higher binding energy is expected if quantum confinement plays a major role. For a 3 nm Si nanocrystal, the ab initio pseudopotential calculations show that the exciton Coulomb energy and the energy gap expansion (as compared to the bulk Si band gap) are ~1.5 and ~1.3 eV, respectively.[22] It has been shown that the core-level shift is consistent with the band-gap expansion.[6] Therefore, one may expect a binding energy shift on the order of ~1 eV due to quantum confinement. The BOLS correlation mechanism also predicts a large binding energy shift of ~1.5 eV for a size of 3 nm.[6,21] Another effect that can lead to a shift to a higher binding energy is dielectric screening of the core hole in the final state.

In the nanocrystal, the hole is surrounded by SiO_2 with a dielectric constant of 3.9, whereas in bulk Si, the hole is surrounded by Si with a dielectric constant of 11.9. Therefore, one can expect a poorer screening in the nanocrystal and thus a higher binding energy. Based on the photoemission-induced charging effect in bulk Si observed in our experiment, the dielectric screening can account for ~0.8 eV of binding energy shift. Obviously, all of the effects mentioned above lead to a core-level shift to a higher binding energy, and thus they cannot explain the result shown in Figure 2.

It is suspected that the correction for the charging effect shown in Figure 2 could have been affected by the differential charging[23,24] between the SiO_2 surface layer and the nc-Si underneath. The redshift is extracted after the correction with the C 1s binding energy due to contamination. The C contamination is most likely residing on the SiO_2 surface and thus can be used to correct for charging in the SiO_2 surface layer. This explains why the core level of the oxidation state of Si^{4+} after the correction for the charging effect is the same as that of pure SiO_2 as shown in Figure 3. However, there is no such internal indicator for the nanocrystals. Recently, it is shown that the differential charging between a SiO_2 layer (1−10 nm) and the underlying Si substrate is as much as 1 eV.[23,24] This has an important implication. As most of the nanocrystals are located at the depths of 3−7 nm underneath the surface, the differential charging could be quite significant. Therefore, using the C 1s for the correction may overestimate the charging in the nanocrystals. Further experimental and theoretical works are required to determine the actual charging in the nanocrystlas and to examine its influence on the core-level shift of the nanocrystals.

In conclusion, the introduction of Si into a SiO_2 thin film enhances the charging effect greatly as compared to the system of a pure SiO_2 thin film grown on a Si substrate. The charging effect has a strong influence on the Si 2p core levels causing the core levels of all oxidation states Si^{n+} (n = 0, 1, 2, 3, and 4) in the material system to shift to a higher binding energy. After the correction for the charging effect, the core level of oxidation state Si^{4+} is the same as that of pure SiO_2. However, the core level of the isolated nc-Si after the correction shifts by ~0.6 eV to a lower binding energy as compared to that of bulk crystalline Si. It is suspected that the core-level shift of the nc-

Si toward a lower binding energy is due to the influence of the differential charging between the SiO_2 surface layer and the nc-Si underneath.

References and Notes

(1) Lalic, N.; Linnros, J. *J. Lumin.* **1999**, *80*, 263.
(2) Kapetanakis, E.; Normand, P.; Tsoukalas, D.; Beltsios, K.; Stoemenos, J.; Zhang, S.; Berg, J. van den *Appl. Phys. Lett.* **2000**, *77,* 3450.
(3) Shi, Y.; Saito, K.; Ishikuro, H.; Hiramoto, T. *J. Appl. Phys.* **1998**, *84,* 2358.
(4) Boer, E. A.; Brongersma, M. L.; Atwater, H. A.; Flagan, R. C.; Bell, L. D. *Appl. Phys. Lett.* **2001**, *79,* 791.
(5) Choi, S. H.; Elliman, R. G. *Appl. Phys. Lett.* **1999**, *75*, 968.
(6) Sun, C. Q.; Pan, L. K.; Fu, Y. Q.; Tay, B. K.; Li, S. *J. Phys. Chem. B* **2003**, *107*, 5113.
(7) Borgohain, K.; Singh, J. B.; Rama Rao, M. V.; Shripathi, T.; Mahamuni, S. *Phys. Rev. B* **2000**, *61*, 11093.
(8) Schmeisser, D.; Böhme, O.; Yfantis, A.; Heller, T.; Batchelor, D. R.; Lundstrom, I.; Spetz, A. L. *Phys. Rev. Lett.* **1999**, *83*, 380.
(9) Yang, D. Q.; Sacher, E. *Appl. Surf. Sci.* **2002**, *195*, 187.
(10) Ohgi, T.; Fujita, D. *Phys. Rev. B* **2002**, *66*, 115410.
(11) Ohgi, T.; Sheng, H.-Y.; Dong, Z.-C.; Nejoh, H.; Fujita, D. *Appl. Phys. Lett.* **2001**, *79*, 2453.
(12) Colvin, V. L.; Alivisatos, A. P.; Tobin, J. G. *Phys. Rev. Lett.* **1991**, *66*, 2786.
(13) Buuren, T. van; Dinh, L. N.; Chase, L. L.; Siekhaus, W. J.; Terminello, L. J. *Phys. Rev. Lett.* **1998**, *80*, 3803.
(14) Liu, Y.; Chen, T. P.; Ng, C. Y.; Tse, M. S.; Fung, S.; Liu, Y. C.; Li, S.; Zhao, P. *Electrochem. Solid-State Lett.* **2004**, *7*, G134.
(15) López, M.; Garrido, B.; Bonafos, C.; Pérez-Rodríguez, A.; Morante, J. R. *Solid-State Electron.* **2001**, *45*, 1495.
(16) Iacona, F.; Lombardo, S.; Campisano, S. U. *J. Vac. Sci. Technol. B* **1996**, *14*, 2693.
(17) Iwata, S.; Ishizaka, A. *J. Appl. Phys.* **1996**, *79*, 6653.
(18) Himpsel, F. J.; McFeely, F. R.; Taleb-Ibrahimi, A.; Yarmoff, J. A.; Hollinger, G. *Phys. Rev. B* **1988**, *38*, 6084.
(19) Grunthaner, P. J.; Hecht, M. H.; Grunthaner, F. J.; Johnson, N. M. *J. Appl. Phys.* **1987**, *61,* 629.
(20) Liu, Y.; Chen, T. P.; Fu, Y. Q.; Tse, M. S.; Hsieh, J. H.; Ho, P. F.; Liu, Y. C. *J. Phys. D: Appl. Phys.* **2003**, *36*, L97.
(21) Sun, C. Q.; Tay, B. K.; Fu, Y. Q.; Li, S.; Chen, T. P.; Bai, H. L.; Jiang, E. Y. *J. Phys. Chem. B* **2003**, *107*, 411.
(22) Ögüt, S.; Chelikowsky, J. R.; Louie, S. G. *Phys. Rev. Lett.* **1997**, *79*, 1770.
(23) Karadas, F.; Ertas, G.; Suzer S. *J. Phys. Chem. B* **2004**, *108*, 1515.
(24) Ulgut, B.; Suzer, S. *J. Phys. Chem. B* **2003**, *107*, 2939.